Nano Energy 40 (2017) 203–213

Contents lists available at ScienceDirect

Nano Energy

journal homepage: www.elsevier.com/locate/nanoen

Full paper

Self-powered triboelectric nanogenerator buoy ball for applications ranging from environment monitoring to water wave energy farm

Qiongfeng Shi[a,b,c,d], Hao Wang[a,b,c,d], Han Wu[a,b,c,d], Chengkuo Lee[a,b,c,d,e,*]

[a] Department of Electrical & Computer Engineering, National University of Singapore, 4 Engineering Drive 3, Singapore 117576, Singapore
[b] Center for Sensors and MEMS, National University of Singapore, 4 Engineering Drive 3, Singapore 117576, Singapore
[c] Hybrid Integrated Flexible Electronic Systems (HIFES) Program, National University of Singapore, #E6-05-04, 5 Engineering Drive 1, Singapore 117608, Singapore
[d] NUS Suzhou Research Institute (NUSRI), Suzhou Industrial Park, Suzhou 215123, PR China
[e] NUS Graduate School for Integrative Science and Engineering, National University of Singapore, Singapore 117456, Singapore

ARTICLE INFO

Keywords:
Triboelectric nanogenerator
Liquid-solid interface triboelectrification
Water wave
Energy harvesting
Ball

ABSTRACT

Water wave is a huge green energy source existing all around the world, but major portion of the water wave energy remains unexplored due to the harsh environment and lack of efficient technologies. Compared to the traditional water wave based electromagnetic generators, triboelectric nanogenerator (TENG) exhibits advantages of simple device configuration, light weight, wide material choice, low cost and easy scalability. In order to further improve the device robustness and efficiency of TENG for water wave energy harvesting, a highly symmetric 3D spherical-shaped water based triboelectric nanogenerator (SWTENG) is proposed here. It has a spherical shell frame with double-layer water based TENG on both its inner surface and outer surface. The SWTENG with water mass inside is ideally suitable for the water wave energy harvesting, since the 3D symmetric structure is more efficient for harvesting energy from random directions and the double-layer water based TENG design is less susceptible to water leakage. Additionally, the SWTENG can also be used for harvesting energy from various energy sources, such as 3D vibration, spinning, rotation and human motions, etc. Furthermore, the SWTENG can work as self-powered fishing sensor or can serve as power source for other sensors in environment monitoring on water surface, such as water temperature, water level, water pollution, etc. Due to the high adaptability and scalability, the SWTENG not only can be used as single energy source or self-powered sensor node, but also can be connected into large-scale network to harvest the wide-area water wave energy towards efficient energy farm.

1. Introduction

Nowadays, the energy source of our daily life is heavily depended on the usage of fossil fuels. But with the fossil fuels running out and the consequent issues (pollution, global warming, climate change, etc.), seeking for new green energy source is becoming more and more impending [1–3]. With more than 70% of the earth surface covered by water, water wave is an enormous green energy source existing all around the world. However, most of the water wave energy remains unexplored due to the harsh water environment and the lack of efficient energy harvesting technologies. Although electromagnetic generators have been developed to convert water wave energy into electricity [4–7], there is still no commercial energy farm demonstrated successfully based on this technology. The main challenges remain in the low energy conversion efficiency of the turbine based generators, complicated instruments, water corrosion and high maintenance cost. Therefore, in search for a more reliable and efficient approach to harvest the huge water wave energy is highly desirable and necessary.

Triboelectric nanogenerator (TENG) based on the triboelectrification (or contact electrification) and electrostatic induction has emerged as a promising energy harvesting technology since 2012 [8]. After that, diverse TENGs have been extensively investigated and demonstrated as an effective approach for harvesting mechanical energy including vibration, human motions, airflow and water wave [9–20]. In comparison to the traditional electromagnetic generators, the emerging TENG technology shows greater advantages benefited from the simple device configuration, light weight, wide material choice, cost effectiveness and easy scalability. Furthermore, large-scale TENG array forming network structure on water surface has been reported to effectively scavenge the wide-area water wave energy and produce significant output power [21–24]. Due to the aforementioned merits, TENG provides a more efficient way to harvest the random and large-scale water wave energy.

* Corresponding author at: Department of Electrical & Computer Engineering, National University of Singapore, 4 Engineering Drive 3, Singapore 117576, Singapore.
E-mail address: elelc@nus.edu.sg (C. Lee).

http://dx.doi.org/10.1016/j.nanoen.2017.08.018
Received 16 June 2017; Received in revised form 11 August 2017; Accepted 12 August 2017
Available online 15 August 2017
2211-2855/

When trying to harvest the water wave energy, three-dimension (3D) structure is more advanced and can function better in the complicated water wave environment [25–31]. Previously developed 3D TENGs for water wave energy harvesting are normally based on the design of an encapsulated structure with solid movable mass to create impact on TENGs on the inner surface. For example, a sealed cubic structure with four TENGs on the inner sidewalls and a movable ball mass is proposed to convert the slow and random water wave energy into electricity [25]. An encapsulated box structure with four wavy-structured TENGs as sidewalls and a free-moving metal ball as movable mass is reported to harvest water wave energy [26]. An enclosed polyhedron structure with 12 sets of multilayer wavy-structured TENGs and a hard ball for water wave energy harvesting is demonstrated [27]. A fully enclosed TENG with a rolling dielectric sphere inside the spherical shell is proposed for low frequency water wave energy harvesting [28]. However, there are three major drawbacks of these reported TENGs as water wave energy harvesters. First of all, water wave with low frequency and random direction/amplitude may not cause sizable acceleration on the movable mass, resulting in low impact force on the TENGs and thereby low output performance. Next, the outer surface of these developed devices is normally wasted due to the conventional TENGs cannot work in the water environment, which greatly hinders the energy conversion efficiency. Last but not least, the performance of the developed TENGs for water wave energy harvesting is highly susceptible to water leakage. Even small amount of water leakage can cause device failure due to the conventional solid-solid interface TENG design.

Water leakage may be fatal for the conventional TENGs, but on the other hand, water itself can function as triboelectric material for power generation in liquid-solid interface TENGs. Recently, liquid-solid interface triboelectrification between polymer and water or liquid metal has been investigated for energy harvesting and self-powered sensing applications [32–43]. TENGs using this phenomenon have received increasing research effort and developed rapidly. But current designs mainly focus on energy harvesting from vibration/water drop and self-powered sensing of ion concentration, pressure, flow rate, etc. Only very limited water based TENGs have been demonstrated for water wave energy harvesting [44–46]. A liquid-solid electrification based thin film TENG with electrode array covered by fluorinated ethylene propylene (FEP) is reported for harvesting energy from ambient water motions [44]. A flexible and area-scalable TENG based on triboelectrification between solid and liquid interface is developed for scavenging kinetic water wave energy [45]. A hybrid TENG by integrating interfacial electrification and impact electrification is proposed for harvesting the electrostatic energy and impact energy from water wave [46]. However, these developed liquid-based TENGs are based on 2D structure designs that are less adaptable in the complicated water environment compared to 3D structure. For example, variation from water wave direction can cause significant output degradation for 2D structure design. On the other hand, liquid-based 3D symmetric structure is expected to be more desirable and effective in the complicated water wave environment and less susceptible to water leakage.

Herein, to address and overcome the drawbacks of the previously developed water wave based TENGs, a highly symmetric 3D spherical-shaped water based triboelectric nanogenerator (SWTENG) is proposed and investigated here. The SWTENG comprises double-layer water based TENG configuration, i.e., both its inner surface and outer surface are in contact with water, which is ideally suitable for water wave energy harvesting. Firstly, water inside as movable mass is an ideal approach for harvesting energy from the low frequency and random direction/amplitude water wave due to its fluidic nature. Even under very subtle perturbation, water mass is able to response and move around with conformal contact on the inner surface for output generation. Secondly, the SWTENG using double-layer water based TENG configuration can greatly enhance the energy conversion efficiency because both the inner and the outer surfaces are effectively utilized. Thirdly, the proposed SWTENG is more robust in harsh environment,

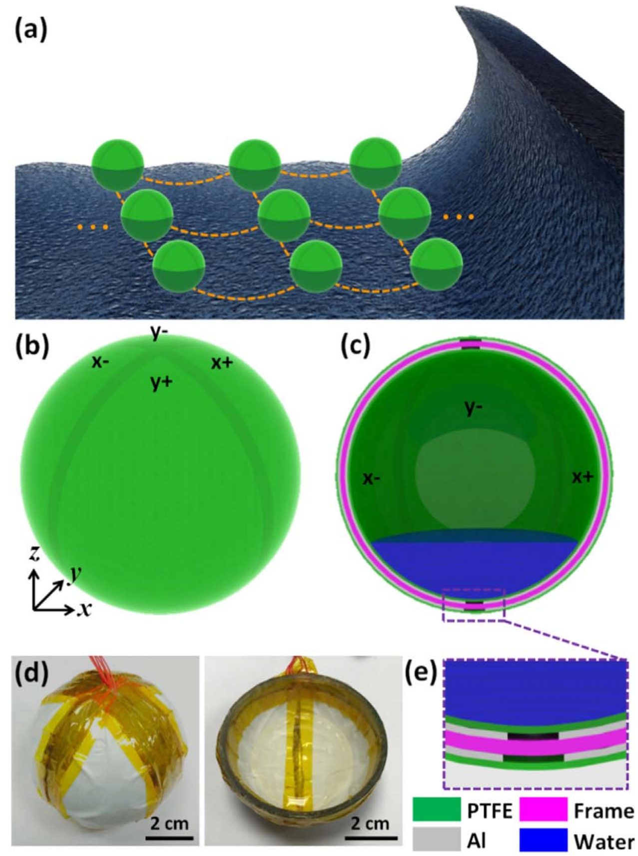

Fig. 1. Device configuration of the SWTENG. (a) Conceptual drawing of the SWTENG array on water surface. (b) Schematic diagram of the proposed SWTENG. (c) Cross-sectional view of the SWTENG. (d) Photograph of the complete SWTENG and the half SWTENG with water mass inside. (e) Enlarged view of the cross sectional structure showing different device layers.

e.g., in underwater and on water surface, and is still able to function well even when water leaks into the encapsulated structure since water is adopted as the triboelectric material. Additionally, the SWTENG can also be used for harvesting energy from 3D vibration, spinning, rotation and diverse human motions. Furthermore, the SWTENG as power source can be integrated with other functional sensors to perform various sensing capabilities. Due to the high scalability, SWTENG array can be connected into network structure on water surface, serving as power source for large-area environment monitoring (e.g. water temperature, water level, water pollution, etc.) and harvesting the huge water wave energy towards efficient water wave energy farm.

2. Device configuration and operation principle

2.1. Symmetric configuration design

Symmetric structure provides a more advanced and effective way to harvest energy from versatile ambient sources including water wave motion, multiple directional vibration, rotating and rolling motion, etc. The device configuration of the proposed symmetric 3D SWTENG is shown in Fig. 1. A conceptual drawing of multiple SWTENGs connected as network array for large-scale water wave energy harvesting is shown in Fig. 1(a). When a random water wave comes along, the SWTENG array will either vibrate up and down or rotate with the water wave, resulting in power generation in large-area. The device configuration of the SWTENG with tilted view and cross-sectional view is illustrated in Fig. 1(b) and (c), respectively. The SWTENG is composed of a spherical shell frame, inner-layer water based TENG with four Al electrodes covered by Polytetrafluoroethylene (PTFE) thin film, outer-layer water based TENG also with four Al electrodes covered by PTFE thin film, and de-ionized (DI) water encapsulated inside as movable mass. The detail schematic diagram of different portions of the SWTENG is depicted in Fig. S1 in the Supplementary Information. Fig. 1(e) is the enlarged view of different layers. Fig. 1(d) shows the photographs of the complete SWTENG and the half SWTENG with water mass. In order to differentiate different electrodes, a coordinate system as shown in Fig. 1(b) is considered as the intrinsic coordinate system of the SWTENG. Then the four inner electrodes are labeled as $E_{in\text{-}x+}$, $E_{in\text{-}y+}$, $E_{in\text{-}x\text{-}}$, $E_{in\text{-}y\text{-}}$ and the four outer electrodes are labeled as $E_{out\text{-}x+}$, $E_{out\text{-}y+}$, $E_{out\text{-}x\text{-}}$, $E_{out\text{-}y\text{-}}$, respectively. $E_{in\text{-}x+}$ and $E_{in\text{-}x\text{-}}$ are then connected as the positive input and negative input of $E_{in\text{-}x}$ while $E_{in\text{-}y+}$ and $E_{in\text{-}y\text{-}}$ are connected as the positive input and negative input of $E_{in\text{-}y}$. For the four outer electrodes, each of them works under single electrode mode to more effectively harvest the random water wave and other ambient mechanical energy.

Fabrication of the SWTENG starts from two hemi-spherical frames with diameter of 6.5 cm which are fabricated by using 3D printing technique with the material of Vero Clear. Then separated and symmetric Al foils are attached on both the inner surface and the outer surface of the two hemi-spherical frames as electrodes. PTFE thin film with thickness of 100 µm is then attached on top of the Al electrodes as the friction layer with water. Kapton tape is adopted to improve the attachment robustness between PTFE thin film and the hemi-spherical frame, and also to prevent water leakage into the Al electrodes. After that, DI water is poured inside one hemi-spherical structure for liquid-solid interface triboelectrification with the inner PTFE thin film. At last, the two hemi-spherical structures are attached and encapsulated together to form the complete SWTENG.

2.2. Operation principle

The SWTENG can be considered as the integration of double-layer water based TENG on the inner surface and outer surface. The operation principle of the inner-layer water based TENG for vibration and spinning/rotating is depicted in Fig. 2(a) and (b), in which only the water mass, inner PTFE and inner electrodes of the SWTENG are shown for simplification. For vibration along x direction, side view of the operation principle is illustrated in Fig. 2(a). Due to difference in electron affiliation ability between PTFE and water, they become negatively charged and positively charged after contacting with each other. After that, when water mass is swung between the left electrode and the right electrode, the induced electrical potential difference drives electrons flow between the two electrodes until new balance is achieved. Thus cyclic output current is generated if the SWTENG is under cyclic vibration. When the SWTENG is vibrating exactly along x direction, only $E_{in\text{-}x}$ generates output current since there is no potential difference in y direction. Vice versa for y direction. If the SWTENG is vibrating at a certain angle with respect to x axis, output current is produced from both $E_{in\text{-}x}$ and $E_{in\text{-}y}$. For spinning/rotating motion, top view of the operation principle is illustrated in Fig. 2(b). When the SWTENG is under spinning/rotating motion, water mass will move along the inner circumference of the SWTENG, creating consecutive electrical potential difference on the four inner electrodes. Then electrons are driven to flow between the two ends of $E_{in\text{-}x}$ and $E_{in\text{-}y}$ in response to the induced electrical potential difference by water mass, resulting in current flow in the external circuit. For the spinning/rotating motion, both of $E_{in\text{-}x}$ and $E_{in\text{-}y}$ produce output current.

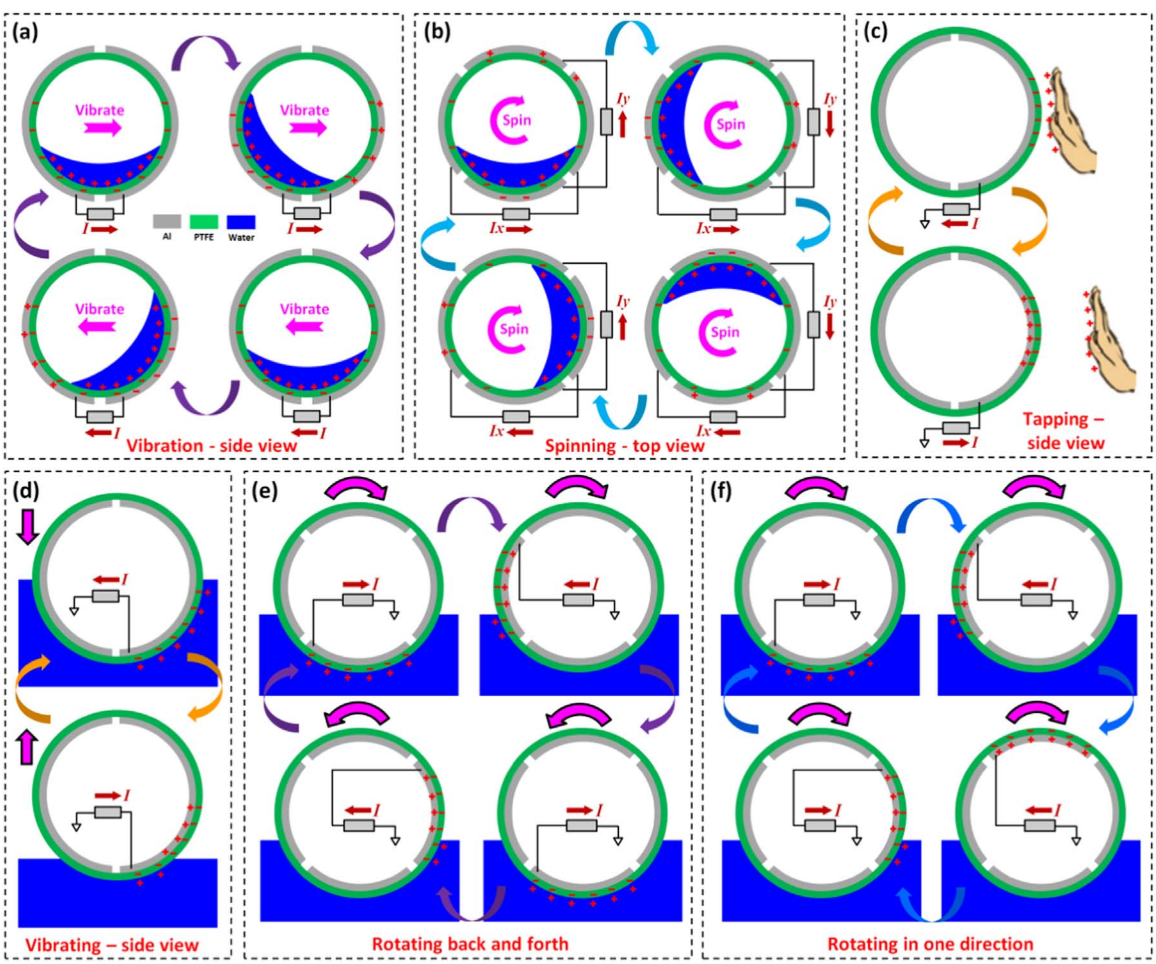

Fig. 2. Operation principle of the SWTENG. Operation principle of the inner-layer TENG under (a) vibration and (b) spinning/rotating motion. Operation principle of the outer-layer TENG under (c) finger tapping, (d) up and down vibration, (e) back and forth rotation and (f) one-direction rotation on water surface.

The operation principle of the outer-layer water based TENG under single electrode mode for harvesting human motion energy and water wave energy is depicted in Fig. 2(c)-(f). Only the outer PTFE and outer electrodes of the SWTENG are shown in the schematic diagram. The operation principle for harvesting energy from human finger tapping is illustrated in Fig. 2(c). PTFE ends up with negative charges on surface and human finger ends up with positive charges on surface after their first contact. Then when human finger is moving closer to the outer-layer TENG, electrons are driven to flow from ground to the Al electrode to balance the electrical potential difference. When human finger is moving away from the outer-layer TENG, electrons are driven to flow from the Al electrode back to ground. Thus current flow between the Al electrode and ground is generated in the external circuit in response to finger tapping. In water wave energy harvesting, there are basically three types of motion that the SWTENG experiences on water surface – vibrating up and down, rotating back and forth, or rotating in one direction. Operation principle of the SWTENG vibrating up and down on water surface is indicated in Fig. 2(d). After contacting, PTFE becomes negatively charged and water surface becomes positively charged. Electrical potential difference is generated when the SWTENG vibrates up and down and water surface level covers to different percentage of the PTFE area. Electrons are driven to flow between the Al electrode and ground, leading to current generation in the external circuit. Operation principle of the SWTENG rotating back and forth or rotating in one direction on the water surface is shown in Fig. 2(e) and (f), respectively. Although water-cover surface level may maintain the same in these two scenarios, electrical potential difference is produced when the PTFE thin film is rotating across the water air interface. Electrons driven by the electrical potential difference are forced to flow between the Al electrode and ground, generating output current flow. In practical situations on water surface for water wave energy harvesting, the actual motion of the SWTENG is normally the combination of these three different motions. Due to the multiple operation principles under different circumstances, the SWTENG has the ability to harvest diverse mechanical energy, human motion energy and random water wave energy from various aspects, enabling high efficiency and good performance under different usage scenarios.

3. Results and discussion

3.1. Device characterization and optimization

Prior to the selection of the dielectric layer for the double-layer water based TENG, a comparison of output performance between Polydimethylsiloxane (PDMS), Kapton and PTFE against water is conducted. As shown in Fig. 3(a), a simple device configuration with metal

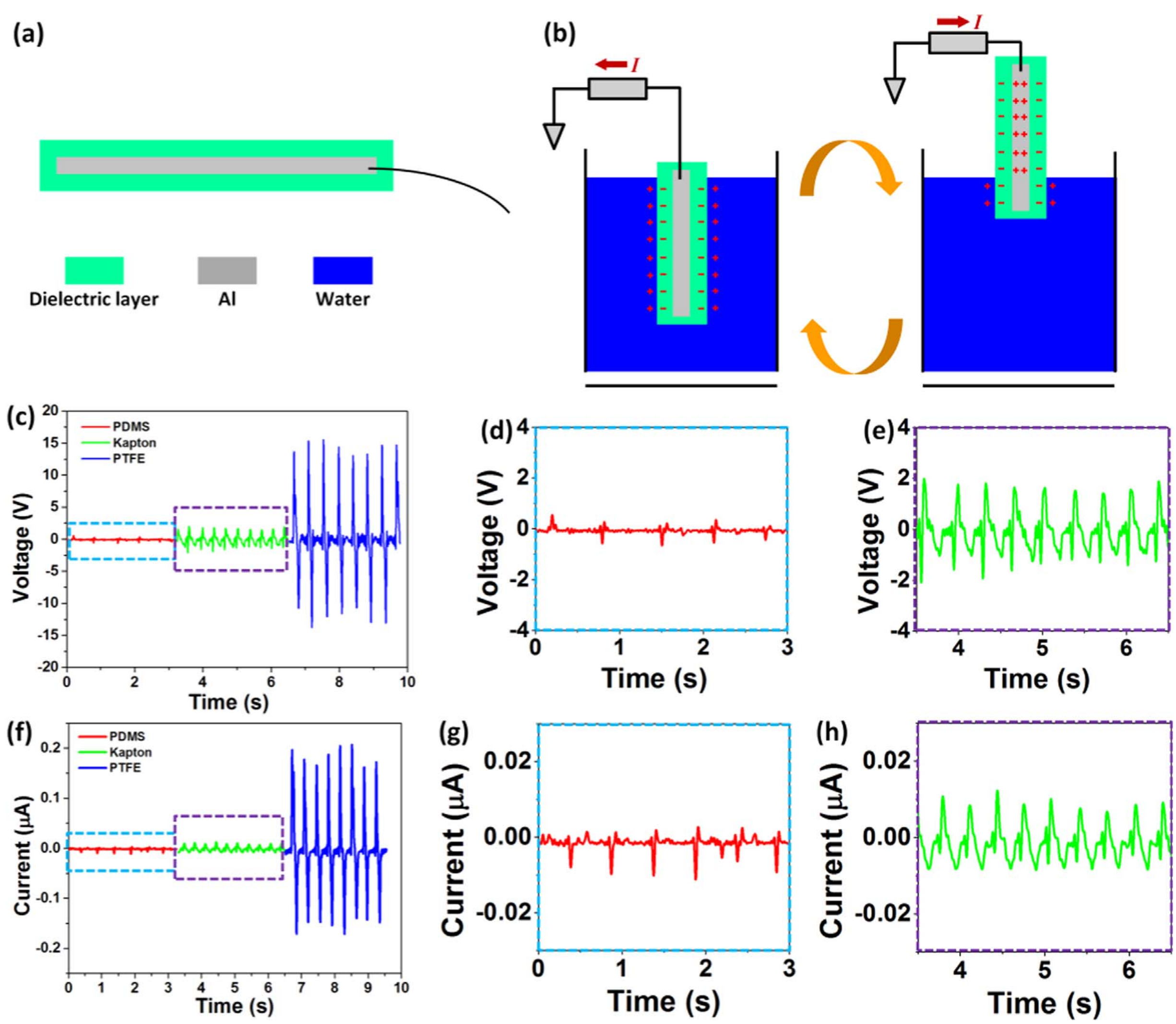

Fig. 3. Characterization of the output performance of different dielectric materials. (a) Device configuration under single electrode mode with different dielectric materials of PDMS, Kapton, PTFE. (b) Operation principle of the device working in a water tank. (c) Output voltage when different dielectric material is adopted. Enlarged view of the output voltage waveform when the dielectric material is (d) PDMS and (e) Kapton. (f) Output current when different dielectric material is adopted. Enlarged view of the output current waveform when the dielectric material is (g) PDMS and (h) Kapton.

electrode coated with dielectric layers on both sides is adopted for the comparison of different materials' performance [37]. With this device configuration, large contact area can be achieved for different dielectric materials and thus the triboelectric performance can be clearly observed and compared. The Al electrode with dimension of 2 cm × 2 cm is sandwiched between the same dielectric layers (PDMS, Kapton or PTFE). The three fabricated devices are then periodically inserted into and pulled out of water for output generation, as illustrated in Fig. 3(b). When the dielectric layer contacts with water, it attracts electrons from water and thus becomes negatively charged on surface while water becomes positively charged. Then when the device is periodically inserted into and pulled out of water, the alternating electrical potential difference drives electrons flow between the Al electrode and ground. The output voltage and current waveform for different dielectric layer is plotted and compared in Fig. 3(c) and (f), respectively. The voltage measurement is achieved by connecting the output to a DSO-X3034A oscilloscope (Agilent) with a high impedance probe of 100 MΩ. The current measurement is achieved by connecting the output to a low noise SR570 current pre-amplifier (Stanford Research Systems). Fig. 3(d) and (e) shows the enlarged voltage waveform for using PDMS and Kapton as the dielectric layer. Fig. 3(g) and (h) shows the enlarged current waveform for using PDMS and Kapton as the dielectric layer. From the output performance, it can be seen that PTFE shows better energy harvesting capability than PDMS and Kapton against water. This can be attributed to its excellent triboelectric property and hydrophobic nature of PTFE thin film, which produces maximum electrical potential difference in water environment. Contact angle measurement of water droplet is conducted by a VCA Optima video contact angle system (AST Products, Inc.), as shown in Fig. S2 in the Supplementary Information. A water droplet of 4 μL is dripped on the surface of Kapton, PDMS and PTFE. The corresponding contact angle is measured to be 97.9°, 111.8° and 111.5°, respectively. For water based TENGs, triboelectric surface with good hydrophobicity is essential since residual water on the triboelectric surface reduces the electrical potential difference and thus weakens the power generation capability. Therefore, PTFE thin film with excellent triboelectric property and hydrophobic nature is selected as the dielectric layer for the water based SWTENG.

As discussed in the operation principle section for the inner-layer water based TENG, water mass can be activated by ambient mechanical excitation such as vibration and spinning motion. Fig. 4(a) depicts the testing setup diagram for vibration along x axis (harmonic vibration) and spinning motion around a circle, where the output voltage from E_{in-x} is measured. The amount of water inside the SWTENG is important on the output performance. Thus the device is first characterized and optimized in terms of the encapsulated water volume ratio. In order to determine the optimized water volume ratio, output voltage from E_{in-x} is measured when water volume ratio varies, as shown in Fig. 4(b). The applied vibration is along x direction with frequency of 3.5 Hz and amplitude of 5 cm. Other than 3.5 Hz vibration, 1 Hz and 2 Hz vibration measurements are also conducted to find out the corresponding optimized water volume ratio. As shown in Fig. 4(c), it can be observed that when the vibration frequency decreases, the overall output performance also decreases due to the lower acceleration. Different frequency seems to have an optimized water volume ratio which decreases

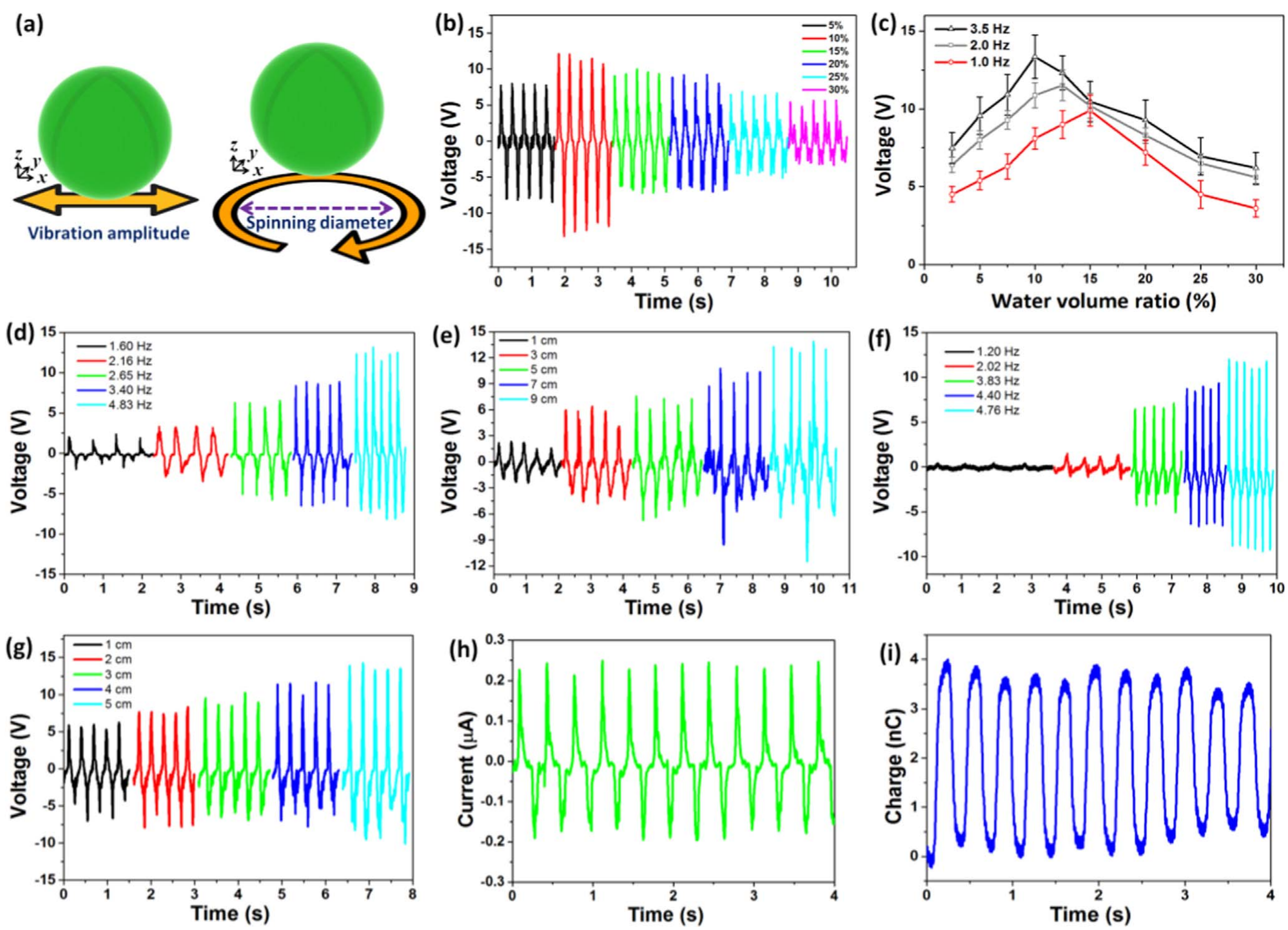

Fig. 4. Device characterization and optimization of the SWTENG. (a) Schematic diagram of the testing setup for vibration and spinning motion. (b) Output voltage from vibration motion with different water volume ratio at 3.5 Hz. (c) Relationship of the output voltage with different water volume ratio at different frequency. Output voltage from vibration motion when (d) different frequency and (e) different amplitude is applied. Output voltage from spinning motion when (f) different frequency and (g) different diameter is applied. (h) Current and (i) charge generated from the inner electrode when the SWTENG is under vibration.

when the vibration frequency increases. This may be due to the fluidic nature of water. When higher frequency is applied, the water is spread out in a large-area and thus covers more surface area. When the frequency reduces, more amount of water is required to cover the same surface area. Here water volume ratio of 10% is adopted for the SWTENG. Then output voltage performance with different vibration frequency is measured and plotted in Fig. 4(d), from 1.6 to 4.8 Hz at 3 cm displacement. Output voltage performance with different vibration displacement amplitude is then measured and shown in Fig. 4(e). The vibration amplitude increases from 1 cm to 9 cm while the vibration frequency is fixed at 2.5 Hz. From these results, it can be observed that the output voltage increases with vibration frequency and amplitude due to the increment of contact area. Although output voltage from both E_{in-x} and E_{in-y} is generated when the SWTENG is under spinning motion, only output from E_{in-x} is measured and plotted to compare with the output from vibration motion. Fig. 4(f) shows the output voltage performance with different spinning frequency when the spinning diameter is fixed at 3 cm. Fig. 4(g) shows the output voltage performance with different spinning diameter when the spinning frequency is maintained at 3.5 Hz. The results show that output voltage

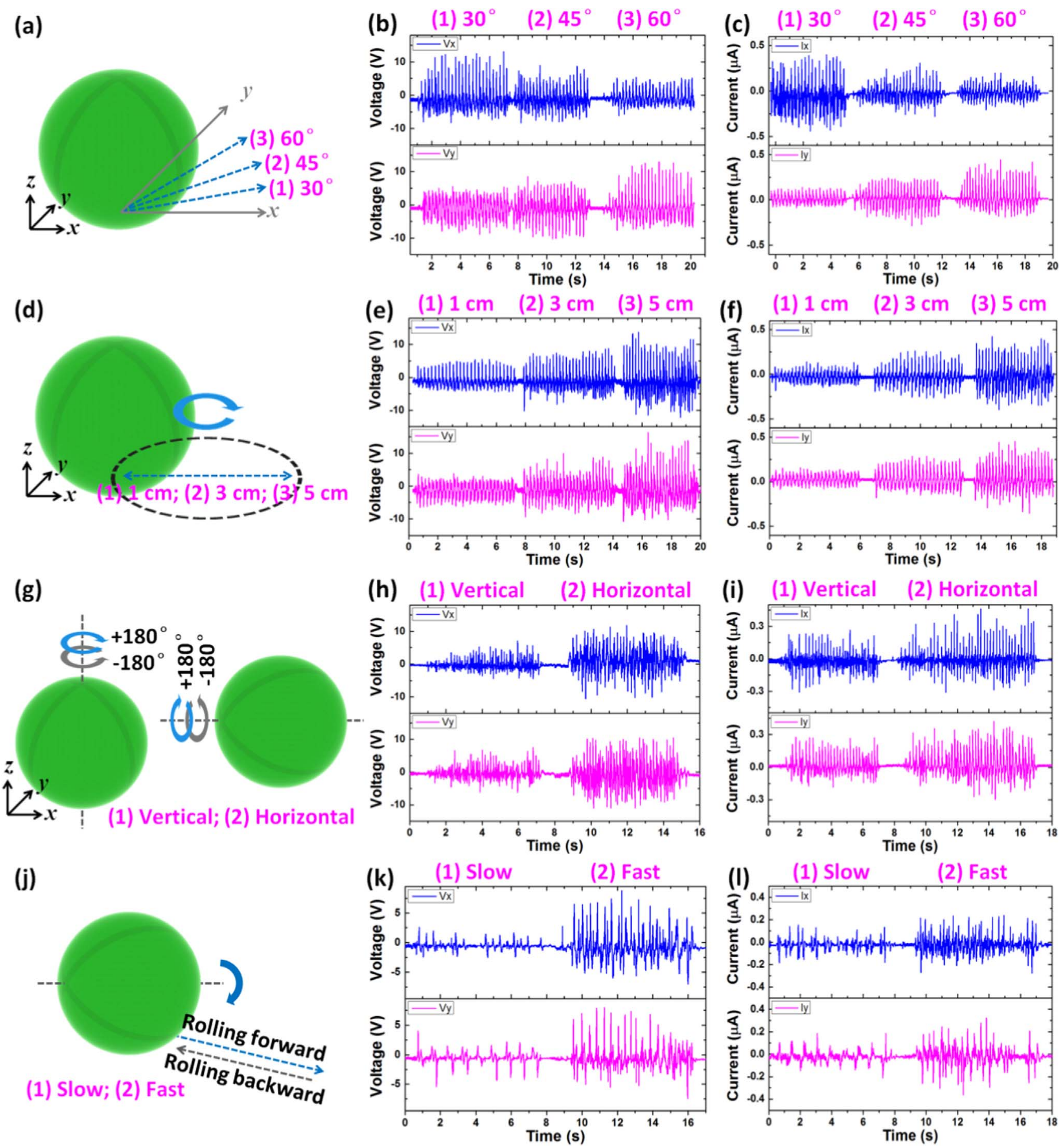

Fig. 5. Energy harvesting capability of the SWTENG under versatile mechanical excitations. (a) Schematic diagram, (b) output voltage and (c) output current when the SWTENG is vibrating along 30°, 45° and 60° with respect to x axis. (d) Schematic diagram, (e) output voltage and (f) output current when the SWTENG is spinning with diameter of 1 cm, 3 cm and 5 cm. (g) Schematic diagram, (h) output voltage and (i) output current when the SWTENG is rotating vertically and horizontally. (j) Schematic diagram, (k) output voltage and (l) output current when the SWTENG is rolling slowly and fast.

increases when the spinning frequency or diameter increases. This is due to the increment of contact area when higher spinning frequency or diameter is applied on the SWTENG. With higher spinning frequency or diameter, higher centripetal force is required for the water mass to maintain the circular motion, hence the water mass is swung higher and spread into large-area on the sidewall of the SWTENG due to its fluidic nature. The detail relationship of the output voltage and water volume ratio, vibration frequency, vibration amplitude, spinning frequency and spinning diameter is shown in Fig. S3 in the Supplementary Information. The short-circuit current and the transferred charge under vibration motion of 3 Hz is shown in Fig. 4(h) and (i), respectively. The transferred charge is measured by connecting the output of the SWTENG to a model 6514 system electrometer (Keithley).

3.2. Versatile mechanical motion and human motion energy harvesting capability

The symmetric structure enables the SWTENG to harvest energy under versatile mechanical motion and human motion. Fig. 5 demonstrates its energy harvesting capability under various mechanical motion excitations - vibration, spinning, rotation and rolling. The output voltage and current from both $E_{in\text{-}x}$ and $E_{in\text{-}y}$ are measured and compared. As shown in Fig. 5(a) to (c), the SWTENG is under in-plane (x-y plane) vibration with vibration angle of 30°, 45° and 60° with respect to x axis. From the output voltage and current results, it can be seen that output from $E_{in\text{-}x}$ is higher when vibration angle is smaller than 45° and output from $E_{in\text{-}y}$ is higher when it is vibration angle is larger than 45°. Similar output performance is generated in $E_{in\text{-}x}$ and $E_{in\text{-}y}$ if the vibration angle is 45°. This can be attributed to different contact area in x and y direction when the vibration angle is different. Fig. 5(d) to (f) shows the SWTENG under spinning motion with diameter of 1 cm, 3 cm and 5 cm. The output from both $E_{in\text{-}x}$ and $E_{in\text{-}y}$ increases with larger spinning diameter since larger contact area is achieved. Similar to spinning, the SWTENG is also able to harvest energy when it rotates along its z axis vertically and horizontally as shown in Fig. 5(g) to (i). It can be seen that higher output is achieve when the SWTENG is rotating with its z axis placed horizontally, as the contact area of water mass with the inner electrode is large in the horizontal placement. Rolling is similar to rotating and the device performance with slow and fast rolling is shown in Fig. 5(j) and (l). Higher output is generated in both $E_{in\text{-}x}$ and $E_{in\text{-}y}$ when the SWTENG is rolling fast. The above demonstration of the SWTENG operating under different mechanical motion shows that it is highly adaptable to various usage scenarios and can harvest energy from diverse ambient energy sources due to its novel structure design. The maximum output voltage and output current attained from the inner-layer TENG is 13.5 V and 0.38 μA, respectively, under spinning motion with 5 cm diameter. Due to its diverse energy harvesting capability, the SWTENG has the potential to function as a

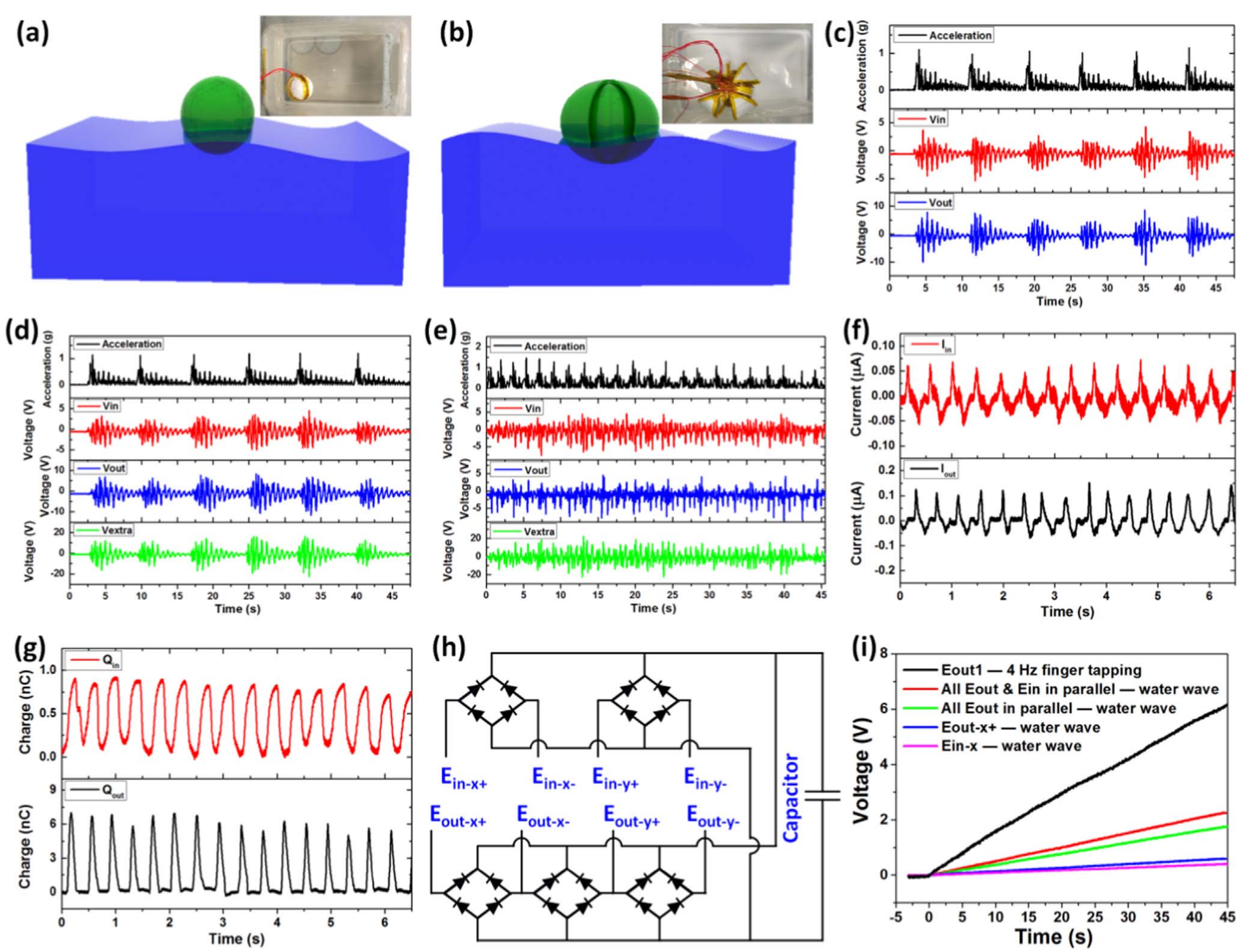

Fig. 6. Water wave energy harvesting by the SWTENG. (a) Schematic diagram of the SWTENG floating on water surface. Insert shows the photograph. (b) Schematic diagram of the enhanced SWTENG. Insert shows the photograph. (c) Output voltage waveform when the SWTENG is excited by 0.15 Hz water wave. (d) Output voltage waveform when the enhanced SWTENG is excited by 0.15 Hz water wave. (e) Output voltage waveform when the enhanced SWTENG is excited by continuous water wave. (f) Current and (g) charge generated from the inner electrode and outer electrode when the SWTENG is excited by continuous water wave. (h) Parallel connection of the multiple outputs after rectification circuit for capacitor charging. (i) Capacitor charging curves by the SWTENG.

self-powered buoy ball on water surface for fishing or other sensing applications. For example, when the SWTENG is connected to a hook and the hook is pulled by a fish, the water mass inside will vibrate along the pulling direction and output signals will be generated. With the x and y direction sensing capability discussed above, pulling force direction or fish position can be differentiated based on the output amplitude in x and y direction.

Fig. S4(a) in the Supplementary Information shows the output voltage and the output power from $E_{in\text{-}x}$ with different external load resistance when the SWTENG is spinning with frequency of 4 Hz and diameter of 5 cm. The maximum power of 3.04 μW can be achieved when the load resistance is 56.5 MΩ. Except for energy harvesting ability from various mechanical motions, the SWTENG can also harvest energy from human motions such as finger tapping. Fig. S4(b) and (c) shows the output voltage and the output current waveform from $E_{out\text{-}x+}$ under single electrode mode when it is cyclically tapped by human finger at frequency of 4 Hz. The output voltage and current achieved is 520 V and 25 μA, respectively. When different external load resistor is connected to the SWTENG, the output voltage and power curve is measured and plotted in Fig. S4(d). The maximum power achieved is 6.5 mW when the load resistance is 9.1 MΩ. The produced output energy from finger tapping can be stored in capacitors after a rectification circuit as power source for other electronics. The charging curves of different capacitors are shown in Fig. S4(e) and (f). The output from the SWTENG by finger tapping can directly light up LED array without using capacitor to store the energy, as depicted in Fig. S4(g) to (i). Video demo of LED array lighting is included in the Supplementary Information Video S1. Additionally, due to the encapsulated movable water mass, the SWTENG can also be used as an inertial sensor for acceleration sensing and human activity monitoring. The relationship of the output voltage from $E_{in\text{-}x}$ and the x-axis acceleration is shown in Fig. S5(a) in the Supplementary Information. When the SWTENG is mounted on human hand, it can serve as a self-powered activity sensor for monitoring different human activities like slow walking, fast walking and running, as shown in Fig. S5(b).

Supplementary material related to this article can be found online at http://dx.doi.org/10.1016/j.nanoen.2017.08.018.

3.3. Water wave energy harvesting

Water wave energy is a huge green energy source existing across the world in oceans, rivers, lakes, pools, etc. However, until now, majority of the water wave energy still remains unexplored and wasted. When trying to harvest the water wave energy, water pollution is one of the main concerns for the water wave energy harvesters. The proposed SWTENG is fabricated from pollution-free materials, i.e. water, Al, PTFE and Vero Clear, thereby providing a green approach to harvest the water wave energy. Furthermore, since water itself is adopted as one triboelectric material, the device is more stable and robust when operating in the wet or water environment. The SWTENG is still able to

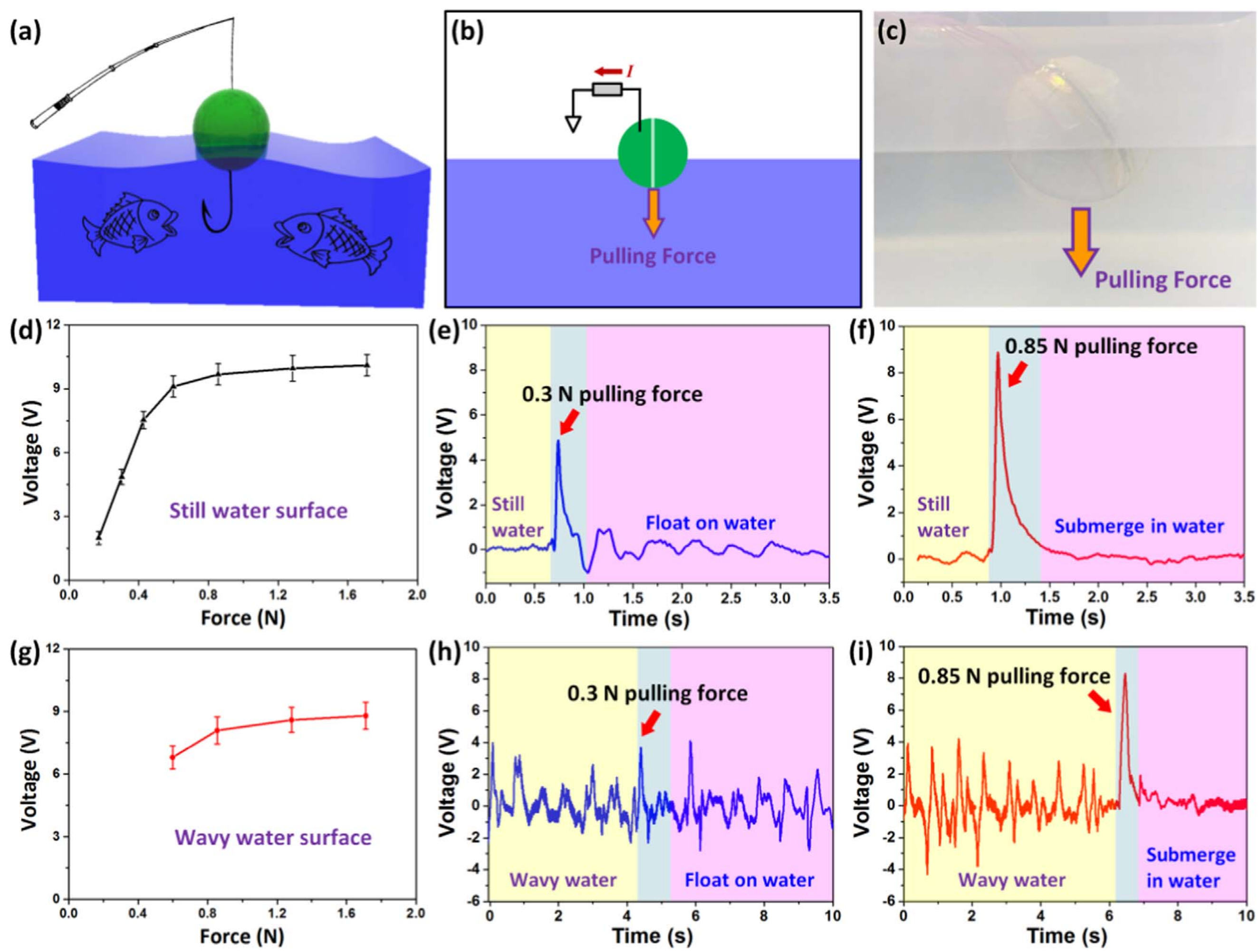

Fig. 7. Demonstration of the SWTENG as a self-powered fishing sensor. (a) Schematic diagram of the SWTENG as a fishing sensor floating on water surface. (b) Testing setup diagram of the SWTENG for pulling force measurement. (c) Photograph of the SWTENG on water surface. (d) Relationship of the output voltage and the applied pulling force on still water surface. Output voltage waveform with (e) 0.3 N and (f) 0.85 N applied force. (g) Relationship of the output voltage and the applied pulling force on wavy water surface. Output voltage waveform with (h) 0.3 N and (i) 0.85 N applied force.

work even when water leakage happens. Thus the proposed SWTENG is ideally suitable for harvesting the ambient water wave energy in a green, stable and efficient way. Multiple SWTENGs can be connected together into network structure to harvest the large-area water wave energy, as depicted in Fig. 1(a). The SWTENG array lying on water surface can also be integrated with other functional sensors to form large-area self-powered sensing system. Each SWTENG node can serve as a power source for the integrated functional sensors to enable self-powered environment monitoring, such as water pollution, water temperature, water level, water flow, etc. Fig. 6(a) shows the schematic diagram and the photograph of the SWTENG floating on water surface as water wave energy harvester. Fig. 6(b) shows an enhanced SWTENG by attaching four additional single electrode water based TENGs on the outer sidewall the SWTENG. The four additional TENGs have the same boat shaped structure with Al electrode covered by PTFE thin film on both sides to enhance the contact area and efficiency. The detail device structure of the enhanced SWTENG is shown in Fig. S6 in the Supplementary Information. More additional TENGs can be further attached layer by layer on the SWTENG forming flower structure to further improve the output performance. As discussed in the operation principle section, the SWTENG will vibrate or rotate on water surface along with the water wave, resulting in power generation from the outer-layer water based TENG. When the SWTENG vibrates or rotates with the water wave, water mass inside the device will also vibrate or rotate on the inner surface, resulting in power generation from the inner-layer water based TENG. The output voltage from the SWTENG and the enhanced SWTENG activated by water wave in a water tank is shown in Fig. 6(c)-(e). A commercial accelerometer ADXL325 (Analog Devices) is attached on the SWTENG and the enhanced SWTENG to measure the actual acceleration magnitude corresponding to the water wave. The output voltage from the electrode $E_{in\text{-}x}$, $E_{out\text{-}x+}$ and $E_{extra\text{-}x+}$ is measured and compared. The water wave in Fig. 6(c) and (d) is produced by shaking the water tank at a low frequency of ~0.15 Hz to mimic the normal ocean wave. The acceleration level and the vertical amplitude of the produced water wave are 1.1 g and 9 cm. The output voltage of the SWTENG is 3.1 V and 7.5 V from $E_{in\text{-}x}$ and $E_{out\text{-}x+}$, respectively. Under similar incoming water wave level, the enhanced SWTENG exhibits similar output voltage from $E_{in\text{-}x}$ and $E_{out\text{-}x+}$, but additional output voltage of 15.2 V is generated from $E_{extra\text{-}x+}$. Higher voltage is generated from $E_{extra\text{-}x+}$ is due to its larger contact area with water from both sides. For the measurement in Fig. 6(e), the water tank is shaken with a higher frequency of ~0.47 Hz to generate the continuous water wave. When the enhanced SWTENG is activated by the continuous water wave, the corresponding voltage output is also generated in a continuous way. The signals in Fig. 6(c) and (e) are magnified and shown in Fig. S7 in the Supplementary Information. When a water wave excitation comes along, the SWTENG will also vibrate with amplitude gradually decreasing. Thus corresponding signals are generated along with the incoming water waves. Then the short-circuit current and the transferred charge from inner electrode and outer electrode under continuous water wave is measured and shown in Fig. 6(f) and (g). Current of 0.07 μA and 0.12 μA and charge of 0.8 nC and 6 nC is observed for inner and outer electrode, respectively. The output energy from water wave activation can also be used for capacitor charging. Output current before and after the rectification circuit is shown in Fig. S8 in the Supplementary Information. A better rectification circuit design for multiple single electrode mode TENGs is adopted [45], and the circuit connection of all the outputs for capacitor charging is shown in Fig. 6(h). The charging curves on a 4.7 μF capacitor from different connection are shown and compared with finger tapping result in Fig. 6(i). The capacitor can be charged up to 2.2 V from parallel connection of the SWTENG after 45 s. Video demo of the SWTENG in the water tank for water wave energy harvesting is shown in the Supplementary Information Video S2.

Supplementary material related to this article can be found online at http://dx.doi.org/10.1016/j.nanoen.2017.08.018.

3.4. Self-powered buoy ball towards water surface sensor

Various sensors are required to operate on water surface in order to collect information of the water pollution, water flow, water level, water temperature, etc. But the harsh and perishable environment makes it quite difficult for regular battery replacement and has high risk to cause battery deterioration and thereby water pollution. On the other hand, the SWTENG buoy ball with diverse energy harvesting capability provides a promising solution, which can function as self-powered sensor on water surface and is robust in the water environment. Moving forward, it can be further optimized and embedded with other sensing function for various sensing applications on the water surface. A self-powered fishing sensor by using the SWTENG as a substitute of fishing buoy is illustrated in Fig. 7(a). The purpose of conventional fishing buoy is to remind the fisherman that there is a fish baiting the hook when it starts to sink. However, sometimes it is not so obvious and one may miss the good chance to pull the fishing rod when he is not fully concentrating. The SWTENG as a self-powered fishing buoy can generate an output signal when fish is pulling the hook, since water air interface for the SWTENG is changed. If the SWTENG is connected with a processing circuit, an alarm signal (e.g. LED flashing) can be triggered. The measurement setup and photograph of the SWTENG floating on the water surface for pulling test is shown in Fig. 7(b) and (c). When there is a pulling force applied on the SWTENG such as fish baiting, it will start to sink into the water. Then an electrical signal is generated on the outer electrode due to the electrical potential difference induced by the water air interface change.

Fig. 7(d) depicts the relationship of the output voltage from $E_{out\text{-}x+}$ and the applied pulling force under still water surface. It can be observed that when the SWTENG is placed on still water surface, the output voltage increases with the applied force. Even when the applied force is as small as 0.2 N, an output voltage peak can be observed. After the applied pulling force exceeds 0.85 N, the output voltage gradually saturated with further increasing the pulling force. The increment of the output voltage is mainly because of the increment of the contact area, i.e. the immersion area of the PTFE thin film due to the applied pulling force. When the pulling force is smaller than 0.85 N, larger immersion area is achieved. But when the pulling force is larger than 0.85 N, the SWTENG is almost all immersed under the water surface and thus the immersion area remains constant after that. The generated output voltage waveform with 0.3 N and 0.85 N applied force is shown in Fig. 7(e) and (f), respectively. The yellow parts of both waveforms show that no signal is generated when the SWTENG is placed on still water surface. Then when force is applied, output peaks with different magnitude are observed. After that, for 0.3 N applied force, since the force is not high enough to pull the device under the water surface, thus the device still floats on the water surface and the agitated water induces small vibrating signals on the device, as shown in the purple part of Fig. 7(e). On the other hand, when for 0.85 N applied force, a higher output voltage peak is generated. Then the device submerges under the water surface completely and no signal is observed after that.

Although fishing on still water surface is common, sometimes fishing on wavy water surface (river or ocean) is also common. To characterize the influence of the wavy water surface, pulling force measurement on wavy water surface with continuous water wave is also conducted. Fig. 7(g) depicts the relationship of the output voltage from $E_{out\text{-}x+}$ and the applied pulling force under wavy water surface. It can be seen that when the SWTENG is placed on wavy water surface, output voltage (~4 V) is already generated even when no pulling force is applied due to the agitated water. Thus if the applied force is too small, the generated voltage peak will be too small to be differentiated from the background signal. When the applied force is larger than 0.6 N, the generated peak can be observed. Typical waveform of 0.3 N and 0.85 N applied force is shown in Fig. 7(h) and (i), respectively. The yellow parts of both waveforms show a background signal without any applied forces. Then when force is applied, output peaks with different magnitude are generated. For 0.3 N applied force, the generated signal is difficult to be differentiated from the background signal. After that, background signal is observed again since the device still floats on water surface. While for 0.85 N applied force, the generated signal is higher than the background signal and can be clearly observed. And after that, no more background signal is observed since the device submerges under the water surface completely. Based on the magnitude of the output signal and the waveform pattern, the SWTENG is able to function as a fishing sensor to monitor the pulling force even under wavy water surface. A demonstration of the SWTENG as self-powered fishing sensor by real fish pulling and the corresponding generated signal are shown in Fig. S9 and Video S3 in the Supplementary Information. In the practical fishing sensor application, the output voltage can be connected to a signal processing circuit for output pattern differentiation. Thereby the information of the fishing environment (still water or wavy water) and the pulling force (larger than a threshold) can be obtained. Then an alarm signal such as LED flashing can be triggered to remind the fisherman that there is a fish pulling the bait. Based on the magnitude of the pulling force, different level of signals can be activated such as one LED flashing, two LED flashing, etc.

Supplementary material related to this article can be found online at http://dx.doi.org/10.1016/j.nanoen.2017.08.018.

4. Conclusion

In summary, a highly symmetric 3D spherical-shaped water based triboelectric nanogenerator (SWTENG) is proposed for harvesting energy from ambient water wave motions and various mechanical motions. The SWTENG with double-layer water based TENG configuration on both surfaces is ideally suitable for harvesting the random directional and irregular water wave energy, due to the novel 3D symmetric structure design and robust water based operation principle. In addition, the SWTENG shows excellent performance for harvesting energy from diverse ambient motions, e.g. 3D vibration, spinning, rotation, rolling and various human motion, etc. Furthermore, the SWTENG can serve as a self-powered fishing sensor on still water surface or wavy water surface to generate a reminding signal when fish pulling the bait. Due to the high adaptability and scalability, the SWTENG not only can function as single power source, but also can form SWTENG network on water surface for large-area water wave energy harvesting towards applications of environment monitoring and efficient water wave energy farm.

Acknowledgement

The authors acknowledge the financial support from the following research grants: Ministry of Education (MOE) Faculty Research Committee (FRC) grant (R-263-000-B56-112) “Thermoelectric Power Generator (TEG) Based Self-Powered ECG Plaster – System Integration (Part 3)” at the National University of Singapore; HIFES seed grant "Hybrid Integration of Flexible Power Source and Pressure Sensors" at the National University of Singapore; NRF-CRP8-2011-01 grant (R-263-000-A27-281) “Self-Powered Body Sensor Network for Disease Management and Prevention Oriented Healthcare” by the National Research Foundation (NRF), Singapore.

Appendix A. Supporting information

Supplementary data associated with this article can be found in the online version at http://dx.doi.org/10.1016/j.nanoen.2017.08.018.

References

[1] J. Glaser, Clean Technol. Environ. 9 (2007) 249–252.
[2] K.S. Brown, Science 285 (1999) 678–680.
[3] D. Clery, Science 320 (2008) (1574-1574).
[4] J. Cruz, Ocean Wave Energy: Current Status and Future Perspectives, Springer Science & Business Media, 2007.
[5] L. Drouen, J. Charpentier, E. Semail, S. Clenet, in: Proceedings of the 2007 IEEE OCEANS, 2007, pp. 1–6.
[6] A. Von Jouanne, Mech. Eng. -CIME 128 (2006) 24–28.
[7] A. Wolfbrandt, IEEE Trans. Magn. 42 (2006) 1812–1819.
[8] F.-R. Fan, Z.-Q. Tian, Z.L. Wang, Nano Energy 1 (2012) 328–334.
[9] Z.L. Wang, J. Chen, L. Lin, Energy Environ. Sci. 8 (2015) 2250–2282.
[10] S. Wang, L. Lin, Z.L. Wang, Nano Energy 11 (2015) 436–462.
[11] M. Shi, H. Wu, J. Zhang, M. Han, B. Meng, H. Zhang, Nano Energy 32 (2017) 479–487.
[12] Q. Zheng, B. Shi, F. Fan, X. Wang, L. Yan, W. Yuan, S. Wang, H. Liu, Z. Li, Z.L. Wang, Adv. Mater. 26 (2014) 5851–5856.
[13] R.K. Gupta, Q. Shi, L. Dhakar, T. Wang, C.H. Heng, C. Lee, Sci. Rep. 7 (2017) 41396.
[14] H.-J. Choi, J.H. Lee, J. Jun, T.Y. Kim, S.-W. Kim, H. Lee, Nano Energy 27 (2016) 595–601.
[15] J. Tian, H. Feng, L. Yan, M. Yu, H. Ouyang, H. Li, W. Jiang, Y. Jin, G. Zhu, Z. Li, Z.L. Wang, Nano Energy 36 (2017) 241–249.
[16] X. Wang, Y. Yang, Nano Energy 32 (2017) 36–41.
[17] T. Li, J. Zou, F. Xing, M. Zhang, X. Cao, N. Wang, Z.L. Wang, ACS Nano 11 (2017) 3950–3956.
[18] D. Bhatia, W. Kim, S. Lee, S.W. Kim, D. Choi, Nano Energy 33 (2017) 515–521.
[19] Q. Zheng, B. Shi, Z. Li, Z.L. Wang, Adv. Sci. 4 (2017) 1700029.
[20] S. Lee, H. Wang, Q. Shi, L. Dhakar, J. Wang, N.V. Thakor, S.-C. Yen, C. Lee, Nano Energy 33 (2017) 1–11.
[21] Z.L. Wang, Faraday Discuss. 176 (2015) 447–458.
[22] Z.L. Wang, Nature 542 (2017) 159–160.
[23] Z.L. Wang, Mater. Today 20 (2017) 74–82.
[24] Z.L. Wang, T. Jiang, L. Xu, Nano Energy 39 (2017) 9–23.
[25] J. Chen, J. Yang, Z. Li, X. Fan, Y. Zi, Q. Jing, H. Guo, Z. Wen, K.C. Pradel, S. Niu, ACS Nano 9 (2015) 3324–3331.
[26] T. Jiang, L.M. Zhang, X. Chen, C.B. Han, W. Tang, C. Zhang, L. Xu, Z.L. Wang, ACS Nano 9 (2015) 12562–12572.
[27] L.M. Zhang, C.B. Han, T. Jiang, T. Zhou, X.H. Li, C. Zhang, Z.L. Wang, Nano Energy 22 (2016) 87–94.
[28] X. Wang, S. Niu, Y. Yin, F. Yi, Z. You, Z.L. Wang, Adv. Energy Mater. 5 (2015) 1501467.
[29] A. Ahmed, Z. Saadatnia, I. Hassan, Y. Zi, Y. Xi, X. He, J. Zu, Z.L. Wang, Adv. Energy Mater. 7 (2017) 1601705.
[30] Y. Zi, H. Guo, Z. Wen, M.-H. Yeh, C. Hu, Z.L. Wang, ACS Nano 10 (2016) 4797–4805.
[31] X. Wang, Z. Wen, H. Guo, C. Wu, X. He, L. Lin, X. Cao, Z.L. Wang, ACS Nano 10 (2016) 11369–11376.
[32] Z.H. Lin, G. Cheng, L. Lin, S. Lee, Z.L. Wang, Angew. Chem. Int. Ed. 52 (2013) 12545–12549.
[33] S.-B. Jeon, D. Kim, M.-L. Seol, S.-J. Park, Y.-K. Choi, Nano Energy 17 (2015) 82–90.
[34] S.-B. Jeon, M.-L. Seol, D. Kim, S.-J. Park, Y.-K. Choi, Adv. Electron. Mater. 2 (2016) 1600006.
[35] Z.H. Lin, G. Cheng, S. Lee, K.C. Pradel, Z.L. Wang, Adv. Mater. 26 (2014) 4690–4696.
[36] L. Zheng, Z.-H. Lin, G. Cheng, W. Wu, X. Wen, S. Lee, Z.L. Wang, Nano Energy 9 (2014) 291–300.
[37] W. Tang, T. Jiang, F.R. Fan, A.F. Yu, C. Zhang, X. Cao, Z.L. Wang, Adv. Funct. Mater. 25 (2015) 3718–3725.
[38] D. Choi, S. Lee, S.M. Park, H. Cho, W. Hwang, D.S. Kim, Nano Res. 8 (2015) 2481–2491.
[39] M. Han, B. Yu, G. Qiu, H. Chen, Z. Su, M. Shi, B. Meng, X. Cheng, H. Zhang, J. Mater. Chem. A 3 (2015) 7382–7388.
[40] Q. Shi, H. Wang, T. Wang, C. Lee, Nano Energy 30 (2016) 450–459.
[41] T. Kim, J. Chung, D.Y. Kim, J.H. Moon, S. Lee, M. Cho, S.H. Lee, S. Lee, Nano Energy 27 (2016) 340–351.
[42] X. Zhang, Y. Zheng, D. Wang, Z.U. Rahman, F. Zhou, Nano Energy 30 (2016) 321–329.
[43] S. Lee, J. Chung, D.Y. Kim, J.-Y. Jung, S.H. Lee, S. Lee, ACS Appl. Mater. Interfaces 8 (2016) 25014–25018.
[44] G. Zhu, Y. Su, P. Bai, J. Chen, Q. Jing, W. Yang, Z.L. Wang, ACS Nano 8 (2014) 6031–6037.
[45] X.J. Zhao, G. Zhu, Y.J. Fan, H.Y. Li, Z.L. Wang, ACS Nano 9 (2015) 7671–7677.
[46] Y. Su, X. Wen, G. Zhu, J. Yang, J. Chen, P. Bai, Z. Wu, Y. Jiang, Z.L. Wang, Nano Energy 9 (2014) 186–195.

Qiongfeng Shi received his B.Eng. degree from Department of Electronic Engineering and Information Science at University of Science and Technology of China (USTC) in 2012. He is currently pursuing his Ph.D. degree in the Department of Electrical and Computer Engineering, National University of Singapore (NUS) under the NUS research scholarship. His research interests are focused on energy harvesters and self-powered sensors.

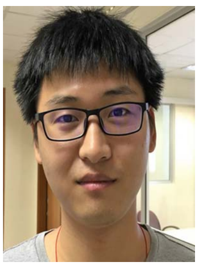

Hao Wang received his B.Eng. degree in School of Optoelectronic Information from University of Electronic Science and Technology of China in 2010. His PhD degree is conferred in Department of Electrical and Computer Engineering (ECE), National University of Singapore (NUS) in Oct 2016. He is currently employed as a Research Fellow in ECE, NUS. His research interests are focused on nanoneedle devices for transdermal drug delivery and triboelectric energy harvester.

Han Wu received his B.Eng. degree in Electronic Science and Technology, M.E. degree in Microelectronics and Solid State Electronics from College of Opto-electronic Engineering, Chongqing University, Chongqing, China, in 2013 and 2016. He is currently working as a research engineer at ECE department of NUS. His research interests include micro energy harvesting, flexible sensors and MEMS actuators & transducers.

Chengkuo Lee received his Ph.D. degree in Precision engineering from The University of Tokyo in 1996. Currently, he is the director of Center for Intelligent Sensors and MEMS, and an Associate Professor in the Department of Electrical and Computer Engineering, National University of Singapore, Singapore. In 2001, he cofounded Asia Pacific Microsystems, Inc., where he was the Vice President. From 2006–2009, he was a Senior Member of the Technical Staff at the Institute of Microelectronics, A-STAR, Singapore. He has contributed to more than 300 international conference papers and extended abstracts and 240 peer-reviewed international journal articles.